Physics and applications of Thomson/Compton back scattering

Camilla Curatolo

October 14, 2013

Thomson/Compton
linear sources
for the production of
high brilliance X/γ rays.

Thomson/Compton
linear sources
for the production of
high brilliance X/γ rays.

Introduction to
Thomson and Compton
back scattering.

Thomson/Compton
linear sources
for the production of
high brilliance X/γ rays.

Introduction to
Thomson and Compton
back scattering.

SPARCLAB
(Pulsed and Amplified Source
of Coherent Radiation LAB)
ELI-NP
(Extreme Light
Infrastructure
Nuclear Physics)

Scattering between relativistic electrons and laser light

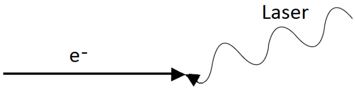

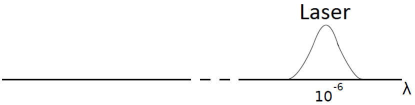

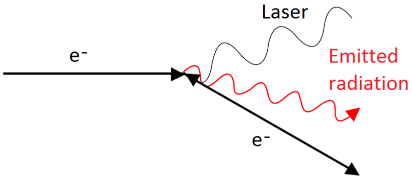

Classical effect

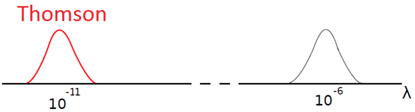

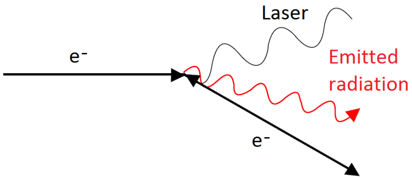

Classical + Quantum effect

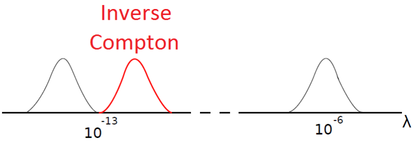

Considering electrons and laser perfectly counterpropagating:

$$\lambda_E = \frac{\lambda_L}{4\gamma^2}$$

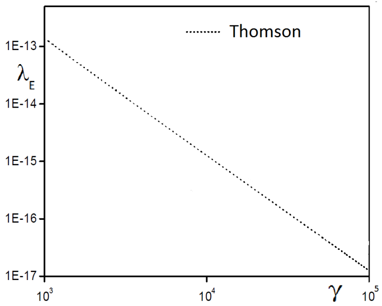

Considering electrons and laser perfectly counterpropagating:

$$\lambda_E = \frac{h}{mc\gamma}$$

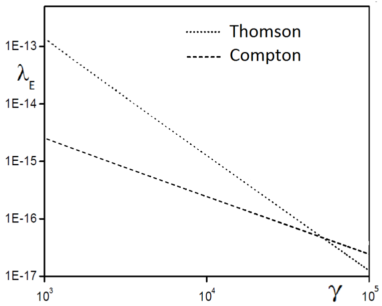

Considering electrons and laser perfectly counterpropagating:

$$\lambda_E = \frac{\lambda_L}{4\gamma^2} + \frac{h}{mc\gamma}$$

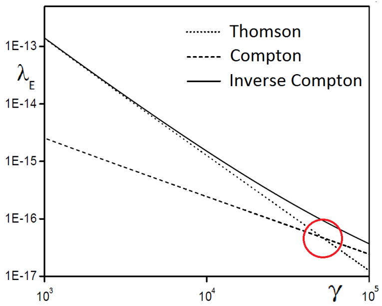

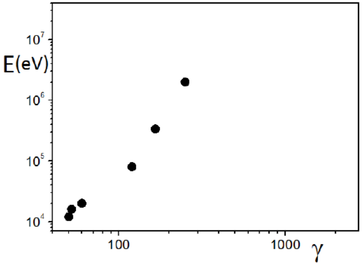

Source	γ	*E*
CLS	50	12 *keV*
PhoeniX	50-60	12-20 *keV*
Pleiades	40-200	20-500 *keV*
SPARCLAB	60-300	20-500 *keV*
LSS (ATF)	240	80 *keV*
FMega-ray	500	2 *MeV*

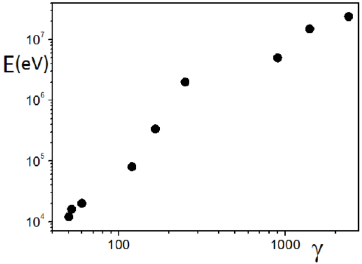

Source	γ	*E*
CLS	50	12 *keV*
PhoeniX	50-60	12-20 *keV*
Pleiades	40-200	20-500 *keV*
SPARCLAB	60-300	20-500 *keV*
LSS (ATF)	240	80 *keV*
FMega-ray	500	2 *MeV*
Hiγs	920	5 *MeV*
ELI-NP	600-1400	5-20 *MeV*
MightyLaser	2400	24 *MeV*

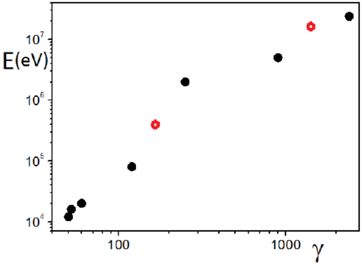

Source	γ	*E*
CLS	50	12 *keV*
PhoeniX	50-60	12-20 *keV*
Pleiades	40-200	20-500 *keV*
SPARCLAB	60-300	20-500 *keV*
LSS (ATF)	240	80 *keV*
FMega-ray	500	2 *MeV*
Hiγs	920	5 *MeV*
ELI-NP	600-1400	5-20 *MeV*
MightyLaser	2400	24 *MeV*

SPARCLAB (Pulsed and Amplified Source of Coherent Radiation LAB) at National Laboratories Frascati (Rome)

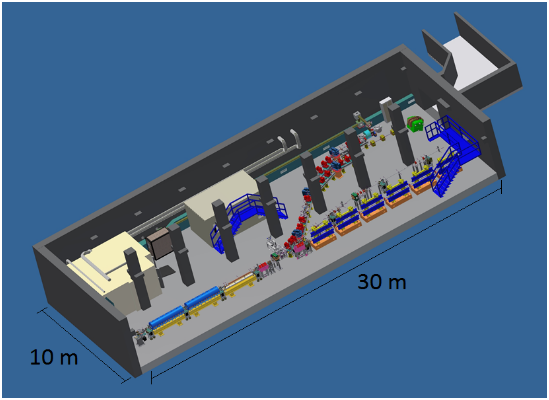

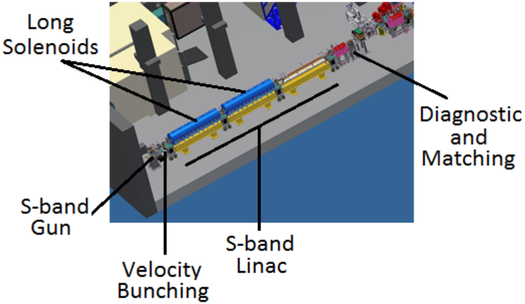

Charge
$$Q = 0.25 - 1 \cdot 10^{-9}\,C$$

Energy
$$E = 30 - 150\ MeV$$

Energy spread
$$\frac{\Delta\gamma}{\gamma} = 7 \cdot 10^{-4}$$

Emittance
$$\epsilon = 0.8 - 1.5\ mm - mrad$$

SPARCLAB

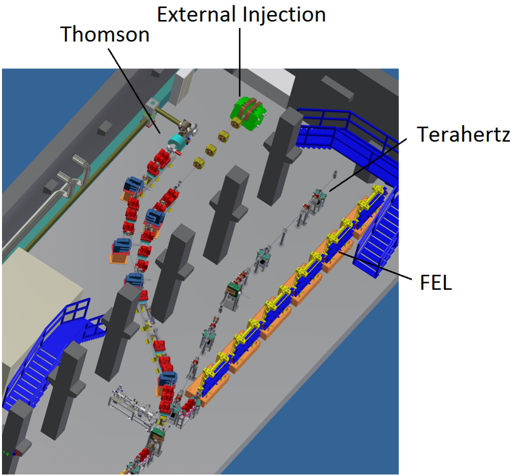

Thomson source

Electrons energy
$E = 30\ MeV$

Laser wavelenght
$\lambda_L = 0.8\ \mu m$

High brilliance X rays
$\lambda_E = 6.2 \cdot 10^{-11}\ m$

Emitted radiation energy
$E_f = 20\ keV$

Number of Photons
$N = 2 \cdot 10^9$

Luminosity
$$L = \frac{N_L N_e}{2\pi(\sigma_x^2 + \frac{w_0^2}{4})} f = 10^{38}\ \frac{1}{sm^2}$$

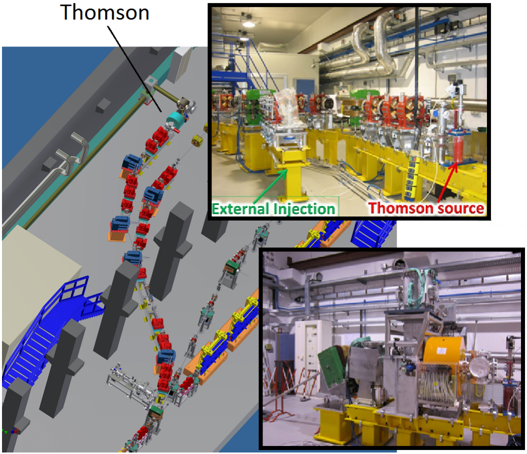

Classical Electrodynamics: from the electron orbits and the Lienard-Wiechert potential in the far zone, the radiation field for one electron is

$$\frac{d^2 W_i}{d\omega d\Omega} = \frac{e^2}{4\pi^2 c}\left|\int_{-\infty}^{+\infty} dt e^{i\omega t}\frac{\vec{n}\times\left[\vec{n}-\vec{\beta}(t')\times\dot{\vec{\beta}}(t')\right]}{(1-\vec{n}\cdot\vec{\beta}(t'))^3}\right|^2 = \hbar\omega\frac{d^2 N_i}{d\omega d\Omega}$$

where $\vec{\beta}$ and $\dot{\vec{\beta}}$ are respectively the velocity and the acceleration of the incoming electron, $\vec{n}$ the direction of the emitted radiation and $t' = t - \frac{1}{c}[\vec{n}r - \vec{r}(t')]$, with $\vec{r}$ position of the electron, is the retarded time.

Classical Electrodynamics: from the electron orbits and the Lienard-Wiechert potential in the far zone, the radiation field for one electron is

$$\frac{d^2 W_i}{d\omega d\Omega} = \frac{e^2}{4\pi^2 c} \left| \int_{-\infty}^{+\infty} dt e^{i\omega t} \frac{\vec{n} \times \left[\vec{n} - \vec{\beta}(t') \times \dot{\vec{\beta}}(t') \right]}{(1 - \vec{n} \cdot \vec{\beta}(t'))^3} \right|^2 = \hbar\omega \frac{d^2 N_i}{d\omega d\Omega}$$

where $\vec{\beta}$ and $\dot{\vec{\beta}}$ are respectively the velocity and the acceleration of the incoming electron, $\vec{n}$ the direction of the emitted radiation and $t' = t - \frac{1}{c}[\vec{n}r - \vec{r}(t')]$, with $\vec{r}$ position of the electron, is the retarded time.

Summing over all of the electrons constituting the beam, we obtain the double differential spectrum $\frac{d^2 N}{d\omega d\Omega}$.

Classical Electrodynamics: from the electron orbits and the Lienard-Wiechert potential in the far zone, the radiation field for one electron is

$$\frac{d^2 W_i}{d\omega d\Omega} = \frac{e^2}{4\pi^2 c} \left| \int_{-\infty}^{+\infty} dt e^{i\omega t} \frac{\vec{n} \times \left[\vec{n} - \vec{\beta}(t') \times \dot{\vec{\beta}}(t') \right]}{(1 - \vec{n} \cdot \vec{\beta}(t'))^3} \right|^2 = \hbar\omega \frac{d^2 N_i}{d\omega d\Omega}$$

where $\vec{\beta}$ and $\dot{\vec{\beta}}$ are respectively the velocity and the acceleration of the incoming electron, $\vec{n}$ the direction of the emitted radiation and $t' = t - \frac{1}{c}[\vec{n}r - \vec{r}(t')]$, with $\vec{r}$ position of the electron, is the retarded time.

Summing over all of the electrons constituting the beam, we obtain the double differential spectrum $\frac{d^2 N}{d\omega d\Omega}$.

Integrating over the solid angle and taking into account the characteristics of the beams we obtain the spectrum of the emitted radiation.

It is very important to predict and evaluate the qualities of the emitted radiation: number of photons, energy, bandwidth, brilliance...

It is very important to predict and evaluate the qualities of the emitted radiation: number of photons, energy, bandwidth, brilliance...

These qualities depend in a critical way from the characteristics of the electron beam: we developed a code, to be implemented directly on the machine, based on a Genetic Algorithm in order to set the optimal parameters of the beam line.

It is very important to predict and evaluate the qualities of the emitted radiation: number of photons, energy, bandwidth, brilliance...

These qualities depend in a critical way from the characteristics of the electron beam: we developed a code, to be implemented directly on the machine, based on a Genetic Algorithm in order to set the optimal parameters of the beam line.

Distincitive feature of this kind of sources is the strong correlation between the emission angle of the radiation and the energy of the emitted photons: from a broad total sprectrum it is possible to select, by using irides or collimators, a highly monochromatic radiation.

The main applications foreseen for the Thomson technology in development at SPARCLAB are advanced imaging techniques for biomedical use.

The main applications foreseen for the Thomson technology in development at SPARCLAB are advanced imaging techniques for biomedical use.

The Thomson source set to produce 20 *keV* X-rays is optimal for mammography:

High monochromaticity → ratio between the signal and the dose absorbed by the patient is much higher than the one of Röntgen tubes.

Reduced dimension → quality of the radiation similar to synchrotron light but the machine is much smaller, easy to install in a hospital.

The main applications foreseen for the Thomson technology in development at SPARCLAB are advanced imaging techniques for biomedical use.

The Thomson source set to produce 20 keV X-rays is optimal for mammography:

High monochromaticity $\rightarrow$ ratio between the signal and the dose absorbed by the patient is much higher than the one of Röntgen tubes.

Reduced dimension $\rightarrow$ quality of the radiation similar to synchrotron light but the machine is much smaller, easy to install in a hospital.

Different settings of the machinary allow to perform fundamental physics experiments: investigate the distribution of the electrons after the scattering.

Thomson at 150 MeV

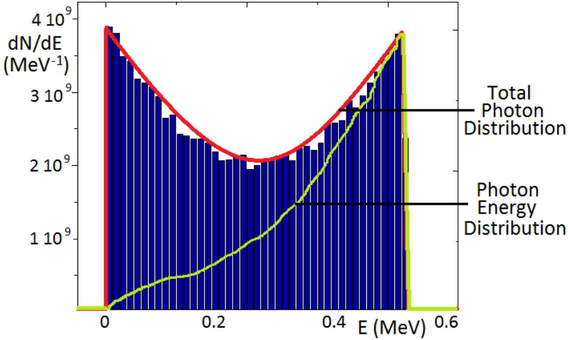

V. Petrillo *et al.*, J. Appl. Phys. **114**, 043104 (2013).

Thomson at 150 MeV

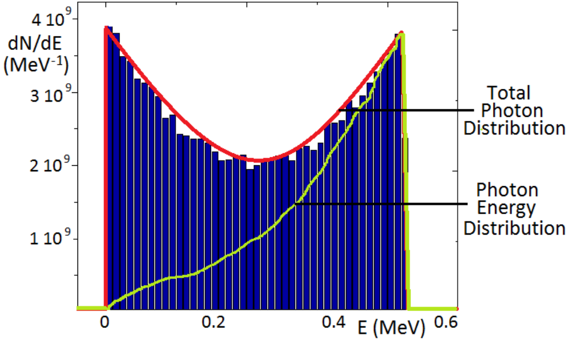

$$\frac{dN_{ph}}{dE} \approx \frac{3}{\Delta E}\left[\left(\frac{E-E_{min}}{\Delta E}\right)^2 - \frac{E-E_{min}}{\Delta E} + \frac{1}{2}\right] \cdot H(E_{max}-E) \cdot H(E-E_{min})$$

V. Petrillo *et al.*, J. Appl. Phys. **114**, 043104 (2013).

Electron distribution P after the scattering.
Model: Chapman-Kolmogorov master equation for Markov processes

$$\frac{\partial P(E,t)}{\partial t} = \alpha \left(\int dE' W(E,E') P(E',t) - P(E,t) \right)$$

with

$$W = \frac{dN_{ph}}{dE}$$

V. Petrillo *et al.*, J. Appl. Phys. **114**, 043104 (2013).

Electron distribution P after the scattering.
Model: Chapman-Kolmogorov master equation for Markov processes

$$\frac{\partial P(E,t)}{\partial t} = \alpha \left(\int dE' W(E,E') P(E',t) - P(E,t) \right)$$

with

$$W = \frac{dN_{ph}}{dE}$$

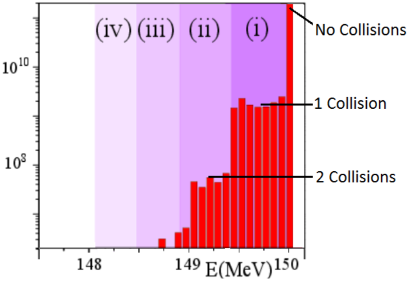

V. Petrillo *et al.*, J. Appl. Phys. **114**, 043104 (2013).

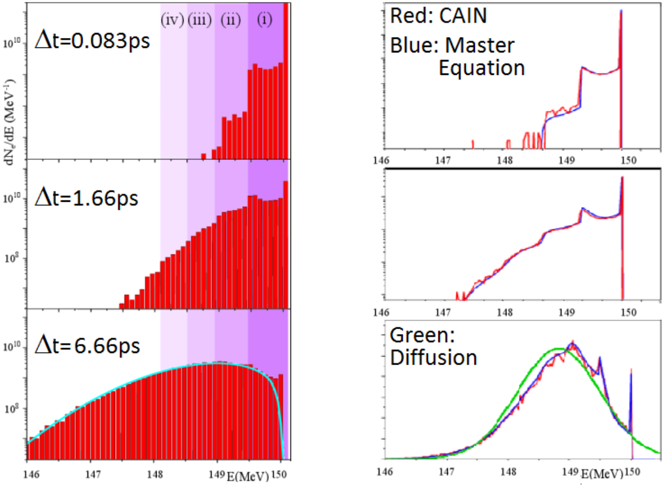

V. Petrillo *et al.*, J. Appl. Phys. **114**, 043104 (2013).

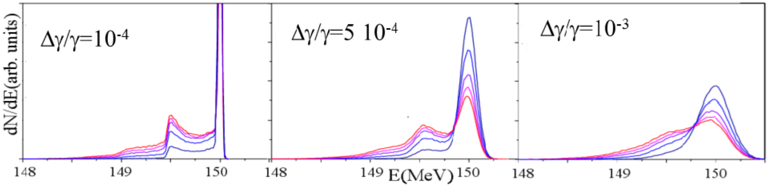

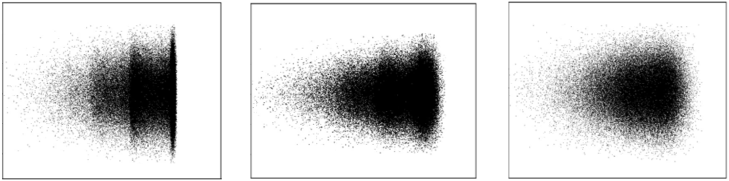

V. Petrillo *et al.*, J. Appl. Phys. **114**, 043104 (2013).

ELI-NP (Extreme Light Infrastructure - Nuclear Physics) to be developed at Magurele (Romania)

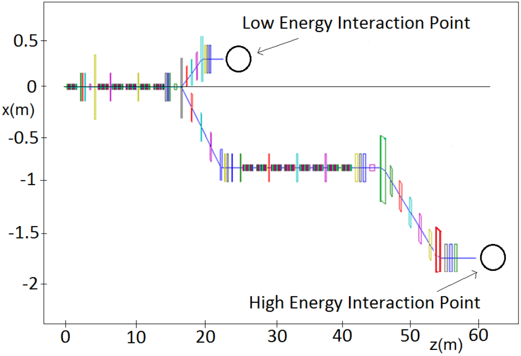

A. Bacci *et al.*, J. App. Phys.l **113**, 194508 (2013).

Electrons energy
$$E = 360 - 720\ MeV$$

Laser wavelenght
$$\lambda_L = 0.5\ \mu m$$

High brilliance γ *rays*
$$\lambda_E = 10^{-13}\ m$$

Emitted radiation energy
$$E_f = 1 - 20\ MeV$$

Number of Photons
$$N = 2 \cdot 10^5$$

Luminosity
$$L = \frac{N_L N_e}{2\pi(\sigma_x^2 + \frac{w_0^2}{4})} f = 10^{39}\ \frac{1}{sm^2}$$

The high energy of the electron beam implies that the recoil of the electrons at the collision is not negligible: theoretical frame is QED.

The high energy of the electron beam implies that the recoil of the electrons at the collision is not negligible: theoretical frame is QED.

Determine the differential Inverse Compton Cross section:
Klein-Nishina + Lorentz transformations or pure QED calculation.

The high energy of the electron beam implies that the recoil of the electrons at the collision is not negligible: theoretical frame is QED.

Determine the differential Inverse Compton Cross section:
Klein-Nishina + Lorentz transformations or pure QED calculation.

Extending to realistic beams and integrating over the solid angle we get the spectrum: the interesting radiation is concentrated in a very narrow angle $\frac{1}{\gamma}$ around the direction of the incoming electron beam.

The high energy of the electron beam implies that the recoil of the electrons at the collision is not negligible: theoretical frame is QED.

Determine the differential Inverse Compton Cross section:
Klein-Nishina + Lorentz transformations or pure QED calculation.

Extending to realistic beams and integrating over the solid angle we get the spectrum: the interesting radiation is concentrated in a very narrow angle $\frac{1}{\gamma}$ around the direction of the incoming electron beam.

Codes: semi-analytical classical non-linear code TSST, semi-analytical quantum code Comp-cross and quantum code CAIN based on a Monte Carlo method.

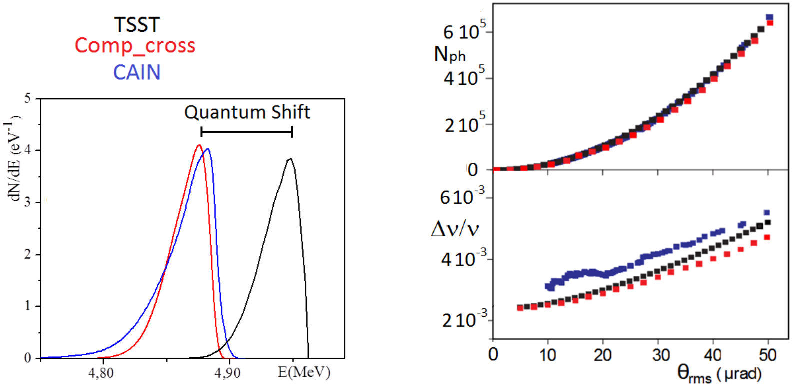

V. Petrillo *et al.*, Nucl. Instrum. Methods Phys. Res. A **693**, 109-116 (2012).

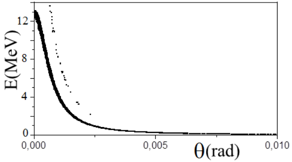
E(MeV)
12
8
4
0
0,000
0,005
0,010
θ(rad)

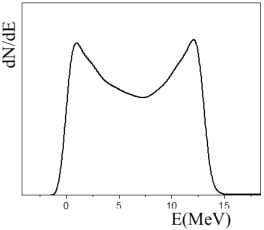
dN/dE
0
5
10
15
E(MeV)

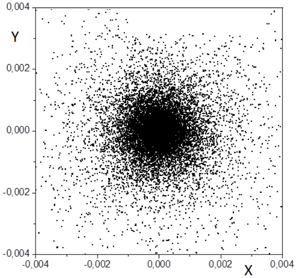
Y
0,004
0,002
0,000
-0,002
-0,004
-0,004
-0,002
0,000
0,002
0,004
X

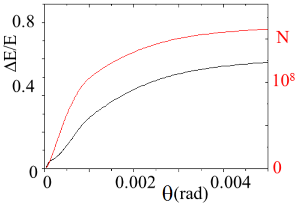
ΔE/E
0.8
0.4
0
0
0.002
0.004
θ(rad)
N
10^8
0

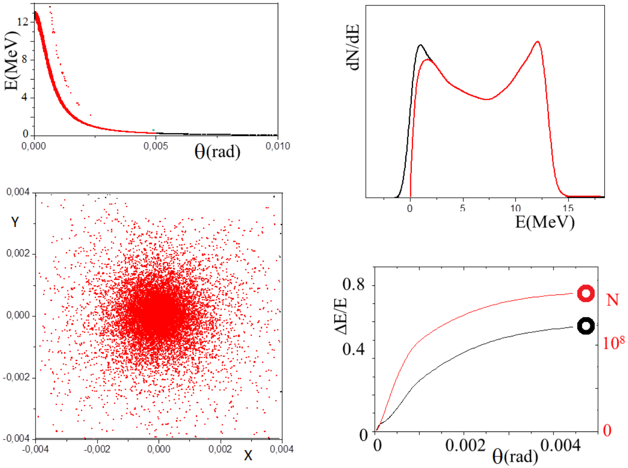
E(MeV)
12
8
4
0
0,000
0,005
θ(rad)
0,010
dN/dE
0
5
10
15
E(MeV)
Y
0,004
0,002
0,000
-0,002
-0,004
-0,004
-0,002
0,000
0,002
X
0,004
ΔE/E
0.8
0.4
0
0
0.002
θ(rad)
0.004
N
10^8
0

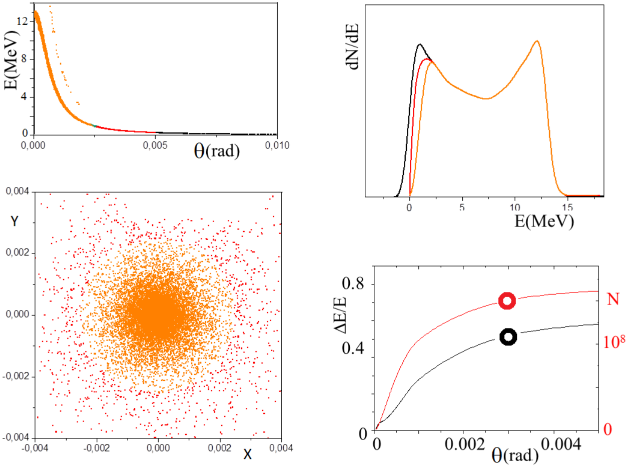
E(MeV)
θ(rad)
0,000
0,005
0,010
12
8
4
0
dN/dE
E(MeV)
0
5
10
15
Y
X
0,004
0,002
0,000
-0,002
-0,004
ΔE/E
0.8
0.4
0
0.002
0.004
N
10⁸

Simulations

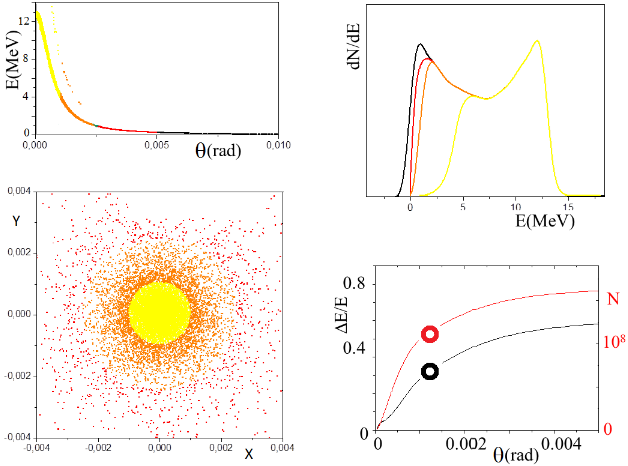

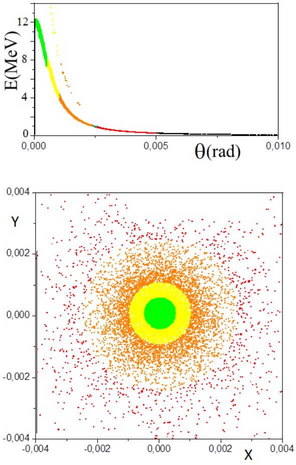

E(MeV)
12
8
4
0
0,000
0,005
θ(rad)
0,010
dN/dE
0
5
10
15
E(MeV)
0,004
Y
0,002
0,000
-0,002
-0,004
-0,004
-0,002
0,000
0,002
X
0,004
ΔE/E
0.8
0.4
0
0
0.002
θ(rad)
0.004
N
10^8
0

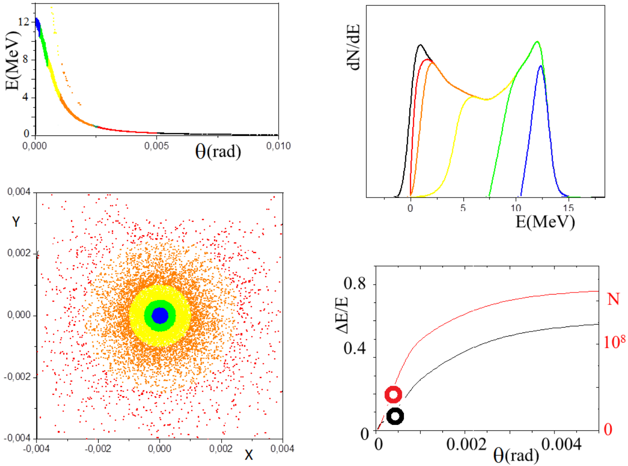
E(MeV)
12
8
4
0
0,000
0,005
θ(rad)
0,010
dN/dE
0
5
10
15
E(MeV)
0,004
Y
0,002
0,000
-0,002
-0,004
-0,004
-0,002
0,000
0,002
X
0,004
ΔE/E
0.8
0.4
0
0
0.002
θ(rad)
0.004
N
10^8
0

SPARCLAB

ELI-NP

Thomson at E = 30 MeV
for 20 KeV X-rays
just started operating

→ Experimental datas
to compare with
theoretical previsions
soon available

SPARCLAB

ELI-NP

SPARCLAB

Thomson at E = 30 MeV
for 20 KeV X-rays
just started operating

Experimental datas
to compare with
theoretical previsions
soon available

Thomson at E =150 MeV
electrons distribution
after scattering

Important for future
e-γ and γ-γ colliders

ELI-NP

SPARCLAB

→ Thomson at E = 30 MeV for 20 KeV X-rays just started operating → Experimental datas to compare with theoretical previsions soon available

→ Thomson at E =150 MeV electrons distribution after scattering → Important for future e-γ and γ-γ colliders

→ Dual color experiment → Pump and probe imaging

ELI-NP

SPARCLAB

Thomson at E = 30 MeV
for 20 KeV X-rays
just started operating

Experimental datas
to compare with
theoretical previsions
soon available

Thomson at E =150 MeV
electrons distribution
after scattering

Important for future
e-γ and γ-γ colliders

Dual color
experiment

Pump and probe
imaging

ELI-NP

Design and optimization
of the accelerator

Sparclab knowledge
(electron Linac)

SPARCLAB	Thomson at E = 30 MeV for 20 KeV X-rays just started operating	Experimental datas to compare with theoretical previsions soon available
	Thomson at E =150 MeV electrons distribution after scattering	Important for future e-γ and γ-γ colliders
	Dual color experiment	Pump and probe imaging
ELI-NP	Design and optimization of the accelerator	Sparclab knowledge (electron Linac)
	Theoretical fundamental issues	Rigorous method to calculate Inverse Compton cross section

SPARCLAB →	Thomson at E = 30 MeV for 20 KeV X-rays just started operating →	Experimental datas to compare with theoretical previsions soon available
	Thomson at E =150 MeV electrons distribution after scattering →	Important for future e-γ and γ-γ colliders
	Dual color experiment →	Pump and probe imaging
ELI-NP →	Design and optimization of the accelerator →	Sparclab knowledge (electron Linac)
	Theoretical fundamental issues →	Rigorous method to calculate Inverse Compton cross section
	Techinical development report May 2013 →	We'll see...

V. Petrillo *et al.*, Nucl. Instrum. Methods Phys. Res. A **693**, 109-116 (2012).

A. Bacci *et al.*, J. App. Phys.l **113**, 194508 (2013).

V. Petrillo *et al.*, J. Appl. Phys. **114**, 043104 (2013).

J. D. Jackson. *Classical Electrodynamics*. John Wiley & Sons, Inc. (1998).

Thank you for your attention!

TABLE I. Summary of gamma-ray beam specifications.

Photon energy	1–20 MeV
Spectral density	$>10^4$ ph/s eV
Bandwidth (rms)	$\leq 0.3\%$
# photons per shot within FWHM bdw.	$2.0–4.0 \cdot 10^5$
# photons/s within FWHM bdw.	$\sim 10^9$
Source rms size	10–30 μm
Source rms divergence	25–250 μrad
Peak brilliance (N_{ph}/s·mm^2 mrad^2·0.1%)	10^{23}–10^{24}
Radiation pulse length (rms, ps)	0.7–1.5
Linear polarization	>95%
Macro rep. rate	100 Hz
# of pulses per macropulse	30–40
Pulse-to-pulse separation	15–20 ns

	E (MeV)	ε_{nx} (μ-rad)	σ_δ (%)	σ_x (μm)	σ_y (μm)
Low energy IP	360	0.4	0.08	14	14
High energy IP	520–720	0.5	0.05	10	10

TABLE III. Electron beam parameters, at the C-band booster injection, for the S-band photo-injector.

	Reference beam (Comp. factor = 2.5)	Commissioning beam (On crest operation)	Commissioning beam (Comp. factor = 2.5)
Charge (pC)	250	25	25
Laser pulse length @ cathode, FWHM (ps)	8.5	3	3
Photocathode laser rms spot size (μm) (uniform transverse distribution)	250	150	150
Output energy (MeV)	79.7	132	79.6
Output RMS Energy spread (%)	1.75	0.02	0.63
Output normalized RMS projected emittance (mm-mrad)	0.4	0.2	0.2
Output RMS bunch length (μm)	280	280	112

Parameter	S-band	C-band
Structure type	Constant gradient, TW	Constant impedance, TW
Working frequency	2.856 GHz	5.712 GHz
Structure length	3 m	1.5 m
Nominal RF input power	40 MW	40 MW
Average accelerating	22 MV/m	35 MV/m
Quality factor	13 000	9000
Shunt impedance per unit length	55 MΩ/m	72 MΩ/m
Filling time	850 ns	230 ns

TABLE II. Laser beam parameters.

Pulse energy (J)	0.5
Wavelength (eV)	2.48
FWHM pulse length (ps)	2–4
Repetition rate (Hz)	100
M^2	$\leq$1.2
Focal spot size w_0 (μm)	>28
Bandwidth (rms)	0.05%
Pointing stability (μrad)	1
Sinchronization to an ext. clock	<1 ps
Pulse energy stability	1%

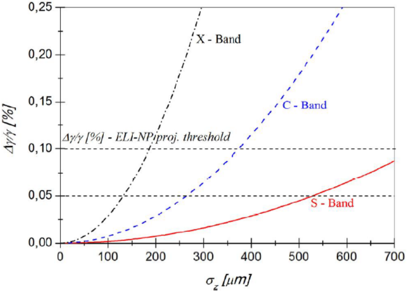

FIG. 3. Energy spread versus bunch length for different RF frequencies: red solid line for the S-band, blue dashed line for C-band, and dashed and dotted black line for X-band. The ELI-NP energy spread maximum threshold is 0.1% and 0.05%; safe values are reported in black dashed lines.

Table 1
Peak-Q energies and dose efficiencies for monochromatic beams, Thomson scattering source and mammographic X-ray tube.

Detail thickness (mm)	Monochromatic beams		Thomson source	X-ray tube
	Peak energy (keV)	Q	Q	Q
1	20.3	0.146	0.137	0.087
2	20.4	0.578	0.547	0.351
5	20.5	3.51	3.34	2.17
10	20.7	13.41	12.75	8.22

Caratteristica	Luce di sincrotrone
Intervallo di energia (keV)	8 - 35
Intervallo energia per esame(keV)	16 - 35
Risoluzione energetica	$\Delta E/E = 2 \times 10^{-3}$
Flusso di fotoni (15 keV)	$2 \times 10^{8}/mm^{-2}s^{-1}$ (2 GeV,300 mA)
Dimensione del fascio (mm)	120×4
Distanza sorgente-campione (m)	≈ 30 (26.5 m nel vuoto)

Tabella 4.1: Caratteristiche del fascio di raggi X prodotto dal sincrotrone

Caratteristica	Luce Thomson
Intervallo di energia (keV)	10 - 150
Intervallo di energia per esame(keV)	16 - 35
Risoluzione energetica	$\Delta E/E = 4 \times 10^{-2}$
Flusso di fotoni a 15 keV	$7 \times 10^{6}/mm^{-2}s^{-1}$
Dimensione del fascio (mm)	$6 \times 6 - 12 \times 12 - 30 \times 30$
Distanza sorgente-campione (m)	$1 - 2 - 5$

Tabella 4.2: Caratteristiche del fascio di raggi X prodotto dalla sorgente Thomson (simulazione)

SPARCLAB: S-band Gun operating at 120 MV/m

$+$

2 S-band TW accelerating cavities,
each 3 m long operating at 22 MV/m

SPARCLAB: S-band Gun operating at 120 MV/m

$+$

2 S-band TW accelerating cavities,
each 3 m long operating at 22 MV/m

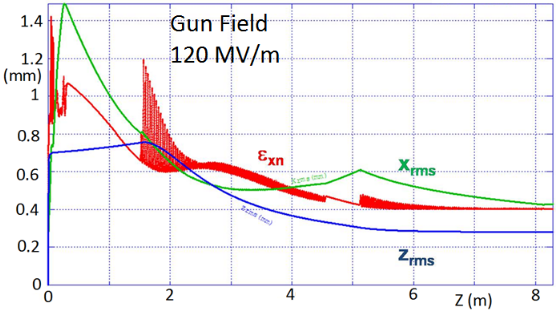

Values at 8 m
ε = 0.407
$\Delta E/E$ = 1.7%
σ_z = 280 μm

A. Bacci *et al.*, J. App. Phys.l **113**, 194508 (2013).

SPARCLAB: S-band Gun operating at 120 MV/m

$+$

2 S-band TW accelerating cavities,
each 3 m long operating at 22 MV/m

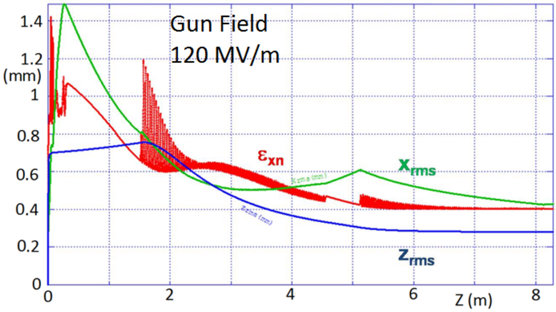

Values at 8 m
ε = 0.407
ΔE/E = 1.7%
σz = 280 μm

A. Bacci *et al.*,
J. App. Phys.l **113**,
194508 (2013).

Same design proposed for ELI-NP.

Study: C-band Gun operating at 170 MV/m

$+$

3 C-band TW accelerating cavities,
each 1.5 m long operating at 35 MV/m

No velocity bunching

Study: C-band Gun operating at 170 MV/m

$+$

3 C-band TW accelerating cavities,
each 1.5 m long operating at 35 MV/m

No velocity bunching

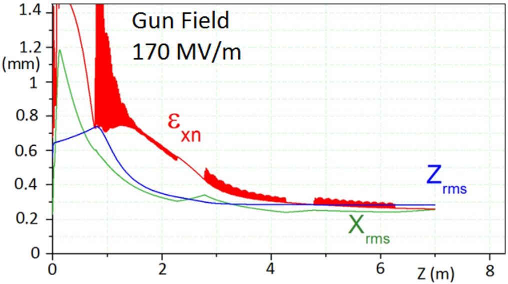

Values at 8 m
$\varepsilon = 0.245$
$\Delta E/E = 0.4\%$
$\sigma_z = 245\ \mu m$

Study: C-band Gun operating at 170 MV/m

$+$

3 C-band TW accelerating cavities,
each 1.5 m long operating at 35 MV/m

No velocity bunching

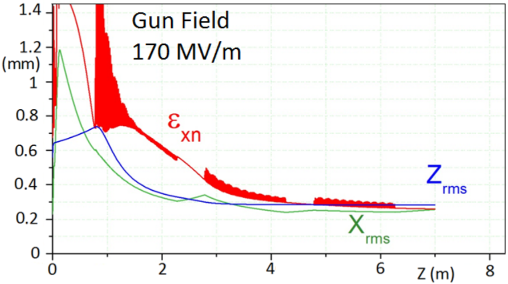

Values at 8 m
$\varepsilon = 0.245$
$\Delta E/E = 0.4\%$
$\sigma_z = 245\ \mu m$

Next SPARCLAB upgrade.

S-band

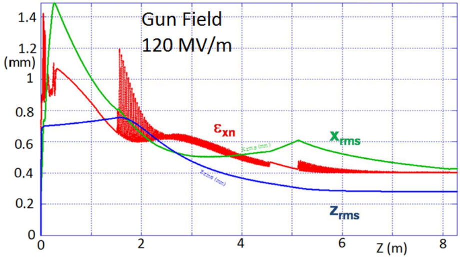

Values at 8 m
$\varepsilon = 0.407$
$\Delta E/E = 1.7\%$
$\sigma_z = 280\ \mu m$

A. Bacci *et al.*, J. App. Phys.l **113**, 194508 (2013).

C-band

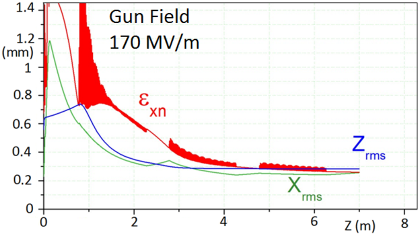

Values at 8 m
$\varepsilon = 0.245$
$\Delta E/E = 0.4\%$
$\sigma_z = 245\ \mu m$

Electron-photon system is described by the initial state

$$|\Psi_{t_1}\rangle = \iint \frac{d^3q'}{q'^0}\frac{d^3k'}{k'^0} e^{\frac{i}{\hbar}(q'^0+k'^0)ct_1} \sum_{r'\lambda'=1}^{2} \Psi_{1e}(q',r')\Psi_{1\gamma}(k',\lambda')\hat{b}^{r'\dagger}(q')\hat{c}^{\lambda'\dagger}(k')|0\rangle$$

Electron-photon system is described by the initial state

$$|\Psi_{t_1}\rangle = \iint \frac{d^3q'}{q'^0}\frac{d^3k'}{k'^0} e^{\frac{i}{\hbar}(q'^0+k'^0)ct_1} \sum_{r'\lambda'=1}^{2} \Psi_{1e}(q',r')\Psi_{1\gamma}(k',\lambda')\hat{b}^{r'\dagger}(q')\hat{c}^{\lambda'\dagger}(k')|0\rangle$$

Transition from $(\vec{q_i},\vec{k_i})$ at t_1 to $(\vec{q_f},\vec{k_f})$ at t_2 with $\Psi_{1e}(q_f,r)\Psi_{1\gamma}(k_f,\lambda) \simeq 0$

Electron-photon system is described by the initial state

$$|\Psi_{t_1}\rangle = \iint \frac{d^3q'}{q'^0}\frac{d^3k'}{k'^0} e^{\frac{i}{\hbar}(q'^0+k'^0)ct_1} \sum_{r'\lambda'=1}^{2} \Psi_{1e}(q',r')\Psi_{1\gamma}(k',\lambda')\hat{b}^{r'\dagger}(q')\hat{c}^{\lambda'\dagger}(k')|0\rangle$$

Transition from $(\vec{q_i},\vec{k_i})$ at t_1 to $(\vec{q_f},\vec{k_f})$ at t_2 with $\Psi_{1e}(q_f,r)\Psi_{1\gamma}(k_f,\lambda) \simeq 0$

$$\hat{E}^{r\lambda}(M) = \iint_M \frac{d^3q}{q^0}\frac{d^3k}{k^0}\hat{b}^{r\dagger}(\vec{q})\hat{c}^{\dagger}_{\lambda}(\vec{k})|0\rangle\langle 0|\hat{c}_{\lambda}(\vec{k})\hat{b}^{r}(\vec{q})$$

$$\sum_{r\lambda}\hat{E}^{r\lambda}(\mathbb{R}^6) = \hat{P}_{e,\gamma}$$

Electron-photon system is described by the initial state

$$|\Psi_{t_1}\rangle = \iint \frac{d^3q'}{q'^0}\frac{d^3k'}{k'^0} e^{\frac{i}{\hbar}(q'^0+k'^0)ct_1} \sum_{r'\lambda'=1}^{2} \Psi_{1e}(q',r')\Psi_{1\gamma}(k',\lambda')\hat{b}^{r'\dagger}(q')\hat{c}^{\lambda'\dagger}(k')|0\rangle$$

Transition from $(\vec{q_i},\vec{k_i})$ at t_1 to $(\vec{q_f},\vec{k_f})$ at t_2 with $\Psi_{1e}(q_f,r)\Psi_{1\gamma}(k_f,\lambda)\simeq 0$

$$\hat{E}^{r\lambda}(M) = \iint_M \frac{d^3q}{q^0}\frac{d^3k}{k^0}\hat{b}^{r\dagger}(\vec{q})\hat{c}^{\dagger}_{\lambda}(\vec{k})|0\rangle\langle 0|\hat{c}_{\lambda}(\vec{k})\hat{b}^{r}(\vec{q})$$

$$\sum_{r\lambda}\hat{E}^{r\lambda}(\mathbb{R}^6) = \hat{P}_{e,\gamma}$$

To calculate the probability $||\hat{E}^{r\lambda}(M)\hat{U}^{inter}(t_2,t_1)\Psi_{t_1}||^2$ we are interested in

$$\Pi^{r\lambda}(\vec{q},\vec{k};t_2,t_1) = |\langle\Phi_{t_2}|\hat{U}^{inter}(t_2,t_1)|\Psi_{t_1}\rangle|^2\frac{1}{k^0q^0}$$

Electron-photon system is described by the initial state

$$|\Psi_{t_1}\rangle = \iint \frac{d^3q'}{q'^0}\frac{d^3k'}{k'^0} e^{\frac{i}{\hbar}(q'^0+k'^0)ct_1} \sum_{r'\lambda'=1}^{2} \Psi_{1e}(q',r')\Psi_{1\gamma}(k',\lambda')\hat{b}^{r'\dagger}(q')\hat{c}^{\lambda'\dagger}(k')|0\rangle$$

Transition from $(\vec{q}_i, \vec{k}_i)$ at t_1 to $(\vec{q}_f, \vec{k}_f)$ at t_2 with $\Psi_{1e}(q_f, r)\Psi_{1\gamma}(k_f, \lambda) \simeq 0$

$$\hat{E}^{r\lambda}(M) = \iint_M \frac{d^3q}{q^0}\frac{d^3k}{k^0} \hat{b}^{r\dagger}(\vec{q})\hat{c}^{\dagger}_{\lambda}(\vec{k})|0\rangle\langle 0|\hat{c}_{\lambda}(\vec{k})\hat{b}^{r}(\vec{q})$$

$$\sum_{r\lambda} \hat{E}^{r\lambda}(\mathbb{R}^6) = \hat{P}_{e,\gamma}$$

To calculate the probability $||\hat{E}^{r\lambda}(M)\hat{U}^{inter}(t_2,t_1)\Psi_{t_1}||^2$ we are interested in

$$\Pi^{r\lambda}(\vec{q},\vec{k};t_2,t_1) = |\langle\Phi_{t_2}|\hat{U}^{inter}(t_2,t_1)|\Psi_{t_1}\rangle|^2 \frac{1}{k^0q^0}$$

$$\langle\Phi_{t_2}|T\left(e^{-\frac{ie}{\hbar c}\int_{ct_1}^{ct_2} dx^0 \int_{\mathbb{R}^3} d^3x :\hat{\bar{\Psi}}(x)\gamma^{\mu}\hat{\Psi}(x)\hat{A}_{\mu}(x):}\right)|\Psi_{t_1}\rangle$$

$$\langle \Phi_{t_2}| - i\left(\frac{e}{\hbar c}\right)^2 \iint_{ct_1}^{ct_2} dx_1^0 dx_2^0 \iint_{\mathbb{R}^3} d^3x_1 d^3x_2 \hat{\overline{\Psi}}^{(-)}(x_2)\gamma^{\mu_2}$$
$$\cdot \left(\hat{A}_{\mu_2}^{(-)}(x_2) S_F(x_2 - x_1)\hat{A}_{\mu_1}^{(+)}(x_1) + \hat{A}_{\mu_1}^{(-)}(x_1) S_F(x_2 - x_1)\hat{A}_{\mu_2}^{(+)}(x_2)\right)\gamma^{\mu_1}\hat{\Psi}^{(+)}(x_1)|\Psi_{t_1}\rangle$$

$$\langle \Phi_{t_2}| - i\left(\frac{e}{\hbar c}\right)^2 \iint_{ct_1}^{ct_2} dx_1^0 dx_2^0 \iint_{\mathbb{R}^3} d^3x_1 d^3x_2 \hat{\overline{\Psi}}^{(-)}(x_2)\gamma^{\mu_2}$$

$$\cdot \left(\hat{A}^{(-)}_{\mu_2}(x_2) S_F(x_2 - x_1)\hat{A}^{(+)}_{\mu_1}(x_1) + \hat{A}^{(-)}_{\mu_1}(x_1) S_F(x_2 - x_1)\hat{A}^{(+)}_{\mu_2}(x_2)\right)\gamma^{\mu_1}\hat{\Psi}^{(+)}(x_1)|\Psi_{t_1}\rangle$$

$$= -\frac{ie^2 m_e}{2}\sum_{r'\lambda'}\iint \frac{d^3q'}{q'^0}\frac{d^3k'}{k'^0} e^{\frac{i}{\hbar}(q'^0+k'^0)ct_1}$$

$$\cdot \iint_{ct_1}^{ct_2} dx_1^0 dx_2^0 \iint_{\mathbb{R}^3} d^3x_1 d^3x_2 \frac{e^{\frac{i}{\hbar}q_f x_2}}{(2\pi\hbar)^{\frac{3}{2}}}\overline{v}^{r_f}(\vec{q_f})\gamma^{\mu_2}$$

$$\cdot \Big[\frac{e^{\frac{i}{\hbar}k_f x_2}}{(2\pi\hbar)^{\frac{3}{2}}} e_{\lambda_f,\mu_2}(\vec{k_f}) S_F(x_2 - x_1)\frac{e^{\frac{i}{\hbar}k' x_1}}{(2\pi\hbar)^{\frac{3}{2}}} e_{\lambda',\mu_1}(\vec{k'})$$

$$+ \frac{e^{\frac{i}{\hbar}k_f x_1}}{(2\pi\hbar)^{\frac{3}{2}}} e_{\lambda_f,\mu_1}(\vec{k_f}) S_F(x_2 - x_1)\frac{e^{-\frac{i}{\hbar}k' x_2}}{(2\pi\hbar)^{\frac{3}{2}}} e_{\lambda',\mu_2}(\vec{k'})\Big]$$

$$\cdot \gamma^{\mu_1} v^{r'}(\vec{q}')\frac{e^{-\frac{i}{\hbar}q' x_1}}{(2\pi\hbar)^{\frac{3}{2}}}\Psi_{1e}(\vec{q'}, r')\Psi_{1\gamma}(\vec{k'}, \lambda')$$

To put in evidence the energy conservation we consider the long time behavior of the system evolution.

To put in evidence the energy conservation we consider the long time behavior of the system evolution.

Since

$$S_F(x) = \lim_{\epsilon \to 0^+} \int dk^0 d^3k \frac{e^{-ikx}}{(2\pi)^4} \frac{k\gamma + \frac{m_e c}{\hbar} I}{k^2 - \frac{m_e^2 c^2}{\hbar^2} + i\epsilon}$$

we integrate on k and develop the calculation of the integral on k^0 utilizing the complex analysis methods.

To put in evidence the energy conservation we consider the long time behavior of the system evolution.

Since

$$S_F(x) = \lim_{\epsilon \to 0^+} \int dk^0 d^3k \frac{e^{-ikx}}{(2\pi)^4} \frac{k\gamma + \frac{m_e c}{\hbar} I}{k^2 - \frac{m_e^2 c^2}{\hbar^2} + i\epsilon}$$

we integrate on k and develop the calculation of the integral on k^0 utilizing the complex analysis methods.

We set the initial wave functions to be peaked around initial momentum $\vec{q}_i$ for the electron and $\vec{k}_i$ for the photon, so that the initial momentum of the particles is in good approximation $\vec{q}_i$ and $\vec{k}_i$.

To put in evidence the energy conservation we consider the long time behavior of the system evolution.

Since

$$S_F(x) = \lim_{\epsilon \to 0^+} \int dk^0 d^3k \frac{e^{-ikx}}{(2\pi)^4} \frac{k\gamma + \frac{m_e c}{\hbar} I}{k^2 - \frac{m_e^2 c^2}{\hbar^2} + i\epsilon}$$

we integrate on k and develop the calculation of the integral on k^0 utilizing the complex analysis methods.

We set the initial wave functions to be peaked around initial momentum $\vec{q}_i$ for the electron and $\vec{k}_i$ for the photon, so that the initial momentum of the particles is in good approximation $\vec{q}_i$ and $\vec{k}_i$.

The wave function of a single particle describes the momentum of the particle through its modulus and is related to the position through the phase. The position of the photon is hardly determined, so it is necessary to take an average over the infinite possible choices of $\vec{x}_0$ in a macroscopic space region ω, inside the bunch, symmetric around the origin, where the density of the photons is constant.

$$P(\lambda_i,\lambda_f,\vec{k_f}\in d\Omega(\theta,\phi)) = \frac{d\Omega(t_2-t_1)c}{V}\frac{e^4 m_e^2}{(4\pi\hbar)^2}\frac{1}{|\vec{k_i}|}\frac{1}{\sqrt{m_e^2c^2+|\vec{q}_i|^2}}$$

$$\cdot\frac{1}{\sqrt{m_e^2c^2+|\vec{q}_i+\vec{k_i}-\vec{k_f}(\theta,\phi)|^2}}\frac{|\vec{k_f}(\theta)|\left(\sqrt{m_e^2c^2+|\vec{q}_i|^2}+|\vec{k_i}|-|\vec{k_f}(\theta)|\right)}{\sqrt{m_e^2c^2+|\vec{q}_i|^2}+k_i-|\vec{q}_i+\vec{k_i}|\cos\theta}$$

$$\cdot Tr_{\mathbb{C}^4}\Big\{\Big[\Big(\not{e}_{\lambda_f}(\vec{k_f}(\theta,\phi))\not{k}_i\not{e}_{\lambda_i}(\vec{k_i})+\not{e}_{\lambda_f}(\vec{k_f}(\theta,\phi))q_i\cdot e_{\lambda_i}(\vec{k_i})\Big)\frac{\hbar}{2q_i\cdot k_i}$$

$$+\Big(\not{e}_{\lambda_i}(\vec{k_i})(-\not{k}_f)\not{e}_{\lambda_f}(\vec{k_f}(\theta,\phi))+\not{e}_{\lambda_i}(\vec{k_i})q_i\cdot e_{\lambda_f}(\vec{k_f}(\theta,\phi))\Big)\frac{\hbar}{-2q_i\cdot k_f(\theta,\phi)}\Big]$$

$$\cdot\frac{1}{2}\Big(\frac{m_ecI+\not{q}_i}{2m_ec}\Big)\cdot\Big[\Big(\not{e}_{\lambda_i}(\vec{k_i})\not{k}_i\not{e}_{\lambda_f}(\vec{k_f}(\theta,\phi))+\not{e}_{\lambda_f}(\vec{k_f}(\theta,\phi))q_i\cdot e_{\lambda_i}(\vec{k_i})\Big)\frac{\hbar}{2q_i\cdot k_i}$$

$$+\Big(\not{e}_{\lambda_f}(\vec{k_f}(\theta,\phi))(-\not{k}_f)\not{e}_{\lambda_i}(\vec{k_i})+\not{e}_{\lambda_i}(\vec{k_i})q_i\cdot e_{\lambda_f}(\vec{k_f}(\theta,\phi))\Big)\frac{\hbar}{-2q_i\cdot k_f(\theta,\phi)}\Big]$$

$$\cdot\frac{m_ecI+\gamma(\vec{q}_i+\vec{k_i}-\vec{k_f}(\theta,\phi))}{2m_ec}\Big\}$$

where $\not{a}=a\cdot\gamma$

$$P(\lambda_i, \lambda_f, \vec{k_f} \in d\Omega(\theta,\phi)) = \frac{d\Omega(t_2 - t_1)c}{V} \frac{e^4 m_e^2}{(4\pi\hbar)^2} \frac{1}{|\vec{k}_i|} \frac{1}{\sqrt{m_e^2c^2 + |\vec{q}_i|^2}}$$

$$\cdot \frac{1}{\sqrt{m_e^2c^2 + |\vec{q}_i + \vec{k}_i - \vec{k_f}(\theta,\phi)|^2}} \frac{|\vec{k_f}(\theta)|\left(\sqrt{m_e^2c^2 + |\vec{q}_i|^2} + |\vec{k}_i| - |\vec{k_f}(\theta)|\right)}{\sqrt{m_e^2c^2 + |\vec{q}_i|^2} + k_i - |\vec{q}_i + \vec{k}_i|\cos\theta}$$

$$\cdot Tr_{\mathbb{C}^4}\Big\{\Big[\Big(\not{e}_{\lambda_f}(\vec{k_f}(\theta,\phi))\not{k}_i\not{e}_{\lambda_i}(\vec{k}_i) + \not{e}_{\lambda_f}(\vec{k_f}(\theta,\phi))q_i \cdot e_{\lambda_i}(\vec{k}_i)\Big)\frac{\hbar}{2q_i \cdot k_i}$$

$$+\Big(\not{e}_{\lambda_i}(\vec{k}_i)(-\not{k}_f)\not{e}_{\lambda_f}(\vec{k_f}(\theta,\phi)) + \not{e}_{\lambda_i}(\vec{k}_i)q_i \cdot e_{\lambda_f}(\vec{k_f}(\theta,\phi))\Big)\frac{\hbar}{-2q_i \cdot k_f(\theta,\phi)}\Big]$$

$$\cdot\frac{1}{2}\Big(\frac{m_e c I + \not{q}_i}{2m_e c}\Big) \cdot \Big[\Big(\not{e}_{\lambda_i}(\vec{k}_i)\not{k}_i\not{e}_{\lambda_f}(\vec{k_f}(\theta,\phi)) + \not{e}_{\lambda_f}(\vec{k_f}(\theta,\phi))q_i \cdot e_{\lambda_i}(\vec{k}_i)\Big)\frac{\hbar}{2q_i \cdot k_i}$$

$$+\Big(\not{e}_{\lambda_f}(\vec{k_f}(\theta,\phi))(-\not{k}_f)\not{e}_{\lambda_i}(\vec{k}_i) + \not{e}_{\lambda_i}(\vec{k}_i)q_i \cdot e_{\lambda_f}(\vec{k_f}(\theta,\phi))\Big)\frac{\hbar}{-2q_i \cdot k_f(\theta,\phi)}\Big]$$

$$\cdot\frac{m_e c I + \gamma(\vec{q}_i + \vec{k}_i - \vec{k_f}(\theta,\phi))}{2m_e c}\Big\}$$

$$
\begin{aligned}
\sigma_{\lambda_i,\lambda_f}(\theta,\phi) &= \frac{e^4 m_e^2}{(4\pi\hbar)^2}\frac{1}{|\vec{k}_i|}\frac{1}{\sqrt{m_e^2c^2+|\vec{q}_i|^2}} \\
&\cdot \frac{1}{\sqrt{m_e^2c^2+|\vec{q}_i+\vec{k}_i-\vec{k}_f(\theta,\phi)|^2}}\frac{|\vec{k}_f(\theta)|\left(\sqrt{m_e^2c^2+|\vec{q}_i|^2}+|\vec{k}_i|-|\vec{k}_f(\theta)|\right)}{\sqrt{m_e^2c^2+|\vec{q}_i|^2}+k_i-|\vec{q}_i+\vec{k}_i|\cos\theta} \\
&\cdot Tr_{\mathbb{C}^4}\Big\{\Big[\Big(\not{e}_{\lambda_f}(\vec{k}_f(\theta,\phi))\not{k}_i\not{e}_{\lambda_i}(\vec{k}_i)+\not{e}_{\lambda_f}(\vec{k}_f(\theta,\phi))q_i\cdot e_{\lambda_i}(\vec{k}_i)\Big)\frac{\hbar}{2q_i\cdot k_i} \\
&+\Big(\not{e}_{\lambda_i}(\vec{k}_i)(-\not{k}_f)\not{e}_{\lambda_f}(\vec{k}_f(\theta,\phi))+\not{e}_{\lambda_i}(\vec{k}_i)q_i\cdot e_{\lambda_f}(\vec{k}_f(\theta,\phi))\Big)\frac{\hbar}{-2q_i\cdot k_f(\theta,\phi)}\Big] \\
&\cdot\frac{1}{2}\Big(\frac{m_e cI+\not{q}_i}{2m_e c}\Big)\cdot\Big[\Big(\not{e}_{\lambda_i}(\vec{k}_i)\not{k}_i\not{e}_{\lambda_f}(\vec{k}_f(\theta,\phi))+\not{e}_{\lambda_f}(\vec{k}_f(\theta,\phi))q_i\cdot e_{\lambda_i}(\vec{k}_i)\Big)\frac{\hbar}{2q_i\cdot k_i} \\
&+\Big(\not{e}_{\lambda_f}(\vec{k}_f(\theta,\phi))(-\not{k}_f)\not{e}_{\lambda_i}(\vec{k}_i)+\not{e}_{\lambda_i}(\vec{k}_i)q_i\cdot e_{\lambda_f}(\vec{k}_f(\theta,\phi))\Big)\frac{\hbar}{-2q_i\cdot k_f(\theta,\phi)}\Big] \\
&\cdot\frac{m_e cI+\gamma(\vec{q}_i+\vec{k}_i-\vec{k}_f(\theta,\phi))}{2m_e c}\Big\}
\end{aligned}
$$

If $\vec{q}_i = 0$ we get the Klein and Nishina formula:

$$(\sigma_{\lambda_i,\lambda_f}(\theta,\phi))_{\vec{q}_i=0} = \frac{1}{4}\left(\frac{e^2}{4\pi m_e c^2}\right)^2 \left(\frac{m_e c}{m_e c + |\vec{k}_i|(1-\cos\theta)}\right)^2$$
$$\cdot\left[4(\vec{e}_{\lambda_f}\cdot\vec{e}_{\lambda_i})^2 + \frac{|\vec{k}_i|^2(1-\cos\theta)^2}{m_e c(m_e c + |\vec{k}_i|(1-\cos\theta))}\right]$$

If $\vec{q}_i = 0$ we get the Klein and Nishina formula:

$$(\sigma_{\lambda_i,\lambda_f}(\theta,\phi))_{\vec{q}_i=0} = \frac{1}{4}\left(\frac{e^2}{4\pi m_e c^2}\right)^2\left(\frac{m_e c}{m_e c + |\vec{k}_i|(1-\cos\theta)}\right)^2 \cdot\left[4(\vec{e}_{\lambda_f}\cdot\vec{e}_{\lambda_i})^2 + \frac{|\vec{k}_i|^2(1-\cos\theta)^2}{m_e c(m_e c + |\vec{k}_i|(1-\cos\theta))}\right]$$

Since $|\vec{k}_i| \ll m_e c$, for not polarized photon beam and not observed polarization of the scattered photons:

$$(\sigma_{\lambda_i,\lambda_f}(\theta,\phi))_{\vec{q}_i=0} = \left(\frac{e^2}{4\pi m_e c^2}\right)^2 \frac{1}{2}(1+\cos^2\theta) = r_0^2\,\frac{(1+\cos^2\theta)}{2}$$

In the general case of $\vec{q}_i \neq 0$ the result is much more complicated:

$$\sigma_{\lambda_i,\lambda_f}(\theta,\phi) = A \cdot B$$

In the general case of $\vec{q}_i \neq 0$ the result is much more complicated:

$$\sigma_{\lambda_i,\lambda_f}(\theta,\phi) = A \cdot B$$

where

$$A = \left(\frac{e^2}{4\pi m_e c^2}\right)^2 \frac{m_e c}{\sqrt{m_e^2 c^2 + |\vec{q}_i|^2}} \frac{m_e c}{\sqrt{m_e^2 c^2 + |\vec{q}_i + \vec{k}_i - \vec{k}_f(\theta,\phi)|^2}}$$
$$\cdot \frac{|\vec{k}_f(\theta)|\left(\sqrt{m_e^2 c^2 + |\vec{q}_i|^2} + |\vec{k}_i| - |\vec{k}_f(\theta)|\right)}{\sqrt{m_e^2 c^2 + |\vec{q}_i|^2} + |\vec{k}_i| - |\vec{q}_i + \vec{k}_i| \cos\theta}$$

$$
\begin{aligned}
B =&\frac{1}{2}\Big\{k_i\cdot k_f\Big[\frac{\vec{q}_i\cdot\vec{e}_{\lambda_f}\vec{e}_{\lambda_f}\cdot\vec{k}_i-\vec{q}_i\cdot\vec{e}_{\lambda_i}\vec{e}_{\lambda_i}\cdot\vec{k}_f}{q_i\cdot k_i q_i\cdot k_f}+\frac{1}{2}\Big(\frac{1}{q_i\cdot k_f}-\frac{1}{q_i\cdot k_i}\Big)\\
&\cdot\Big(1+\frac{(\vec{q}_i\cdot\vec{e}_{\lambda_i})^2}{q_i\cdot k_i}-\frac{(\vec{q}_i\cdot\vec{e}_{\lambda_f})^2}{q_i\cdot k_f}\Big)\Big]+\frac{1}{2}\frac{(\vec{q}_i\cdot\vec{e}_{\lambda_i})^2(\vec{q}_i\cdot\vec{e}_{\lambda_f})^2(q_i\cdot k_i-q_i\cdot k_f)^2}{(q_i\cdot k_i)^2(q_i\cdot k_f)^2}\\
&+2(\vec{e}_{\lambda_i}\cdot\vec{e}_{\lambda_f})^2+\frac{(\vec{q}_i\cdot\vec{k}_f\vec{q}_i\cdot\vec{e}_{\lambda_i}\vec{e}_{\lambda_f}\cdot\vec{k}_i+\vec{q}_i\cdot\vec{k}_i\vec{q}_i\cdot\vec{e}_{\lambda_f}\vec{e}_{\lambda_i}\cdot\vec{k}_f)^2}{(q_i\cdot k_i)^2(q_i\cdot k_f)^2}\\
&+\frac{1}{2}\Big(\vec{q}_i\cdot\vec{e}_{\lambda_f}\vec{e}_{\lambda_f}\cdot\vec{k}_i+\vec{q}_i\cdot\vec{e}_{\lambda_i}\vec{e}_{\lambda_i}\cdot\vec{k}_f+5\vec{q}_i\cdot\vec{e}_{\lambda_i}\vec{q}_i\cdot\vec{e}_{\lambda_f}\vec{e}_{\lambda_i}\cdot\vec{e}_{\lambda_f}\Big)\Big(\frac{1}{q_i\cdot k_i}-\frac{1}{q_i\cdot k_f}\Big)\\
&+\vec{e}_{\lambda_i}\cdot\vec{e}_{\lambda_f}\Big(\frac{\vec{q}_i\cdot\vec{e}_{\lambda_i}\vec{e}_{\lambda_f}\cdot\vec{k}_i}{q_i\cdot k_i}+\frac{\vec{q}_i\cdot\vec{e}_{\lambda_f}\vec{e}_{\lambda_i}\cdot\vec{k}_f}{q_i\cdot k_f}\Big)\\
&+\frac{3}{2}\Big[(\vec{q}_i\cdot\vec{e}_{\lambda_i})^2\vec{q}_i\cdot\vec{e}_{\lambda_f}\vec{e}_{\lambda_f}\cdot\vec{k}_i\Big(\frac{1}{(q_i\cdot k_i)^2}-\frac{1}{q_i\cdot k_i q_i\cdot k_f}\Big)\\
&+\vec{q}_i\cdot\vec{e}_{\lambda_i}(\vec{q}_i\cdot\vec{e}_{\lambda_f})^2\vec{e}_{\lambda_i}\cdot\vec{k}_f\Big(\frac{1}{q_i\cdot k_i q_i\cdot k_f}-\frac{1}{(q_i\cdot k_f)^2}\Big)\Big]\\
&+\frac{1}{4}\Big(\frac{(\vec{q}_i\cdot\vec{e}_{\lambda_i})^2}{(q_i\cdot k_i)^2}+\frac{(\vec{q}_i\cdot\vec{e}_{\lambda_f})^2}{(q_i\cdot k_f)^2}\Big)\Big(q_i\cdot k_i-q_i\cdot k_f\Big)\Big\}
\end{aligned}
$$

Let's consider electron and photon perfectly counterpropagating.

$$|\vec{k_f}(\theta)| = \frac{|\vec{k_i}|\sqrt{m_e^2c^2 + |\vec{q_i}|^2} + |\vec{q_i}||\vec{k_i}|}{|\vec{k_i}| + \sqrt{m_e^2c^2 + |\vec{q_i}|^2} - |\vec{q_i} + \vec{k_i}|\cos\theta}$$

$$|\vec{q_i}| \gg m_e c \gg |\vec{k_i}|$$

$$A \approx \left(\frac{e^2}{4\pi m_e c^2}\right)^2 \frac{8|\vec{q}_i|^2}{m_e^2c^2} \frac{1}{\left(1 + \frac{2|\vec{q}_i|^2}{m_e^2c^2}(1-\cos\theta)\right)^2} = \frac{8r_0^2\gamma^2}{\left(1 + 2\gamma^2(1-\cos\theta)\right)^2}$$

Let's consider electron and photon perfectly counterpropagating.

$$|\vec{k_f}(\theta)| = \frac{|\vec{k_i}|\sqrt{m_e^2c^2 + |\vec{q_i}|^2} + |\vec{q_i}||\vec{k_i}|}{|\vec{k_i}| + \sqrt{m_e^2c^2 + |\vec{q_i}|^2} - |\vec{q_i} + \vec{k_i}|\cos\theta}$$

$$|\vec{q_i}| \gg m_e c \gg |\vec{k_i}|$$

$$A \approx \left(\frac{e^2}{4\pi m_e c^2}\right)^2 \frac{8|\vec{q_i}|^2}{m_e^2 c^2} \frac{1}{\left(1 + \frac{2|\vec{q_i}|^2}{m_e^2 c^2}(1-\cos\theta)\right)^2} = \frac{8 r_0^2 \gamma^2}{\left(1 + 2\gamma^2(1-\cos\theta)\right)^2}$$

$$\begin{array}{cc}
\theta = 0 & A \approx r_0^2 8\gamma^2 \\
\theta < \frac{1}{\gamma} & A \approx 8 r_0^2 \gamma^2 \frac{1}{(1+\gamma^2\theta^2)^2} \\
\theta = \frac{1}{\gamma} & A \approx 2 r_0^2 \gamma^2 \\
\frac{1}{\gamma} < \theta < 1 & A \approx 8 r_0^2 \frac{1}{\gamma^2\theta^4} \\
\theta > 1 & A \approx 2 r_0^2 \frac{1}{\gamma^2(1-\cos\theta)^2}
\end{array}$$

Realizing the sum and the average on the polarization for small θ angles

$$B \approx 1 - \frac{\theta^2}{2} - \Big(\frac{1}{2} - \frac{\theta^2}{4}\Big)\frac{\theta^2}{\theta^2 + \frac{m_e^2 c^2}{|\vec{q}_i|^2}} + \frac{1}{2}\left(\frac{\theta^2}{\theta^2 + \frac{m_e^2 c^2}{|\vec{q}_i|^2}}\right)^2 - \Big(1 - \frac{\theta^2}{4}\Big)\frac{|\vec{k}_i|}{|\vec{q}_i|}\frac{\theta^2}{\theta^2 + \frac{m_e^2 c^2}{|\vec{q}_i|^2}}$$

Realizing the sum and the average on the polarization for small θ angles

$$B \approx 1 - \frac{\theta^2}{2} - \left(\frac{1}{2} - \frac{\theta^2}{4}\right) \frac{\theta^2}{\theta^2 + \frac{m_e^2 c^2}{|\vec{q}_i|^2}} + \frac{1}{2} \left(\frac{\theta^2}{\theta^2 + \frac{m_e^2 c^2}{|\vec{q}_i|^2}} \right)^2 - \left(1 - \frac{\theta^2}{4}\right) \frac{|\vec{k}_i|}{|\vec{q}_i|} \frac{\theta^2}{\theta^2 + \frac{m_e^2 c^2}{|\vec{q}_i|^2}}$$

There is a critical dependence on the angle θ for both A and B.